

Supporting Information

Synergistic Pinning Effect in Layer-structured Oxide Cathode for Enhancing Stability towards Potassium-Ion Batteries

*Xuan-Wen Gao,^{a,b} Shuai-Shuai Wang,^a Qi Li,^a Rui Yang,^a Zhaomeng Liu,^{a,b} Wen-Bin Luo**

^aInstitute for Energy Electrochemistry and Urban Mines Metallurgy, School of Metallurgy, Northeastern University, Shen yang, Liaoning 110819, China.

^bKey Laboratory of Advanced Energy Materials Chemistry (Ministry of Education), College of Chemistry, Nankai University, Tianjin 300071, China

Corresponding Authors

E-mail: luowenbin@smm.neu.edu.cn

KEYWORDS

Potassium ion battery; layer-structured oxide; cathode materials; structural stability; phase transformation

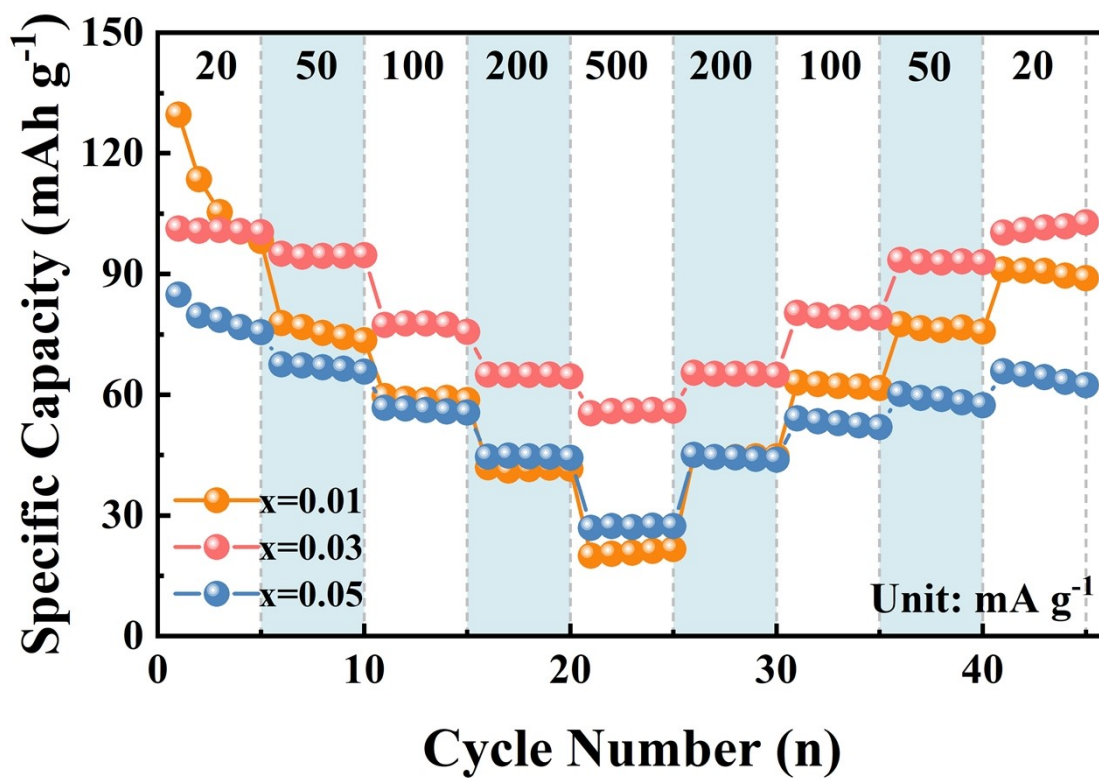


Figure S1. Rate performance comparison of $\text{K}_{0.5}\text{Mn}_{0.9-x}\text{Co}_{0.05}\text{Fe}_{0.05}\text{Li}_x\text{O}_2$ ($x = 0.01, 0.03, 0.05$).

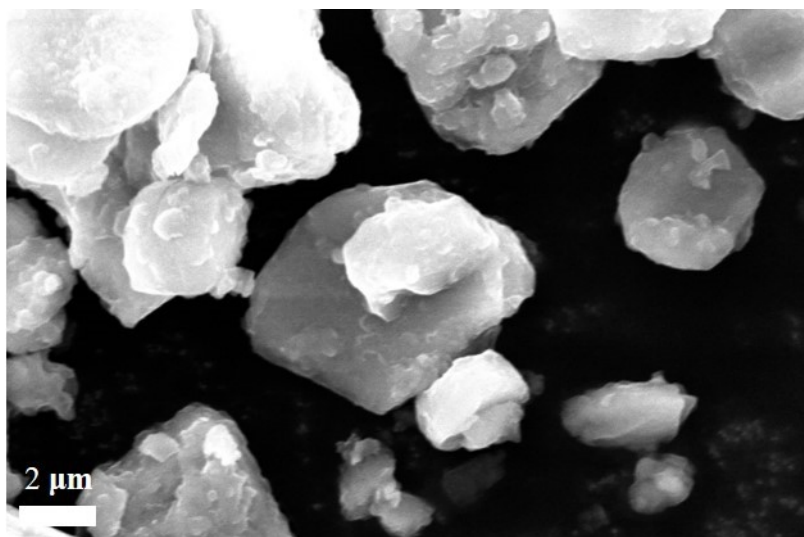


Figure S2. SEM image of KMCFO.

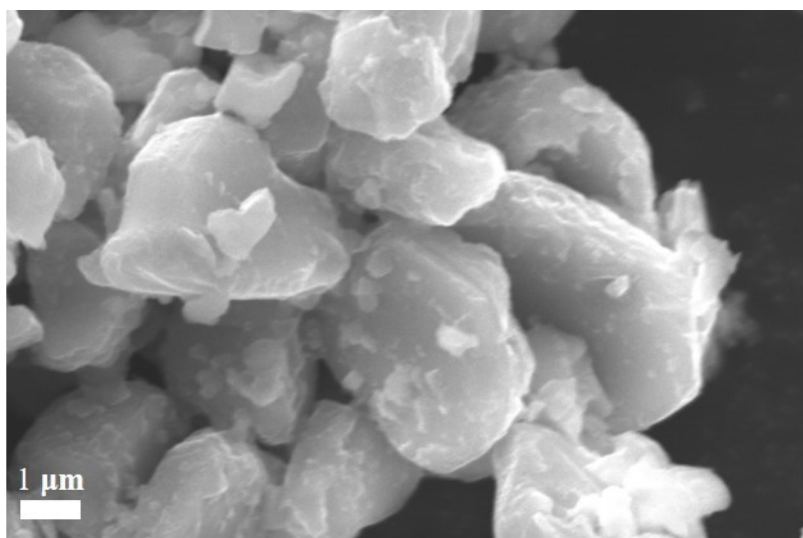


Figure S3. SEM image of KMCFO.

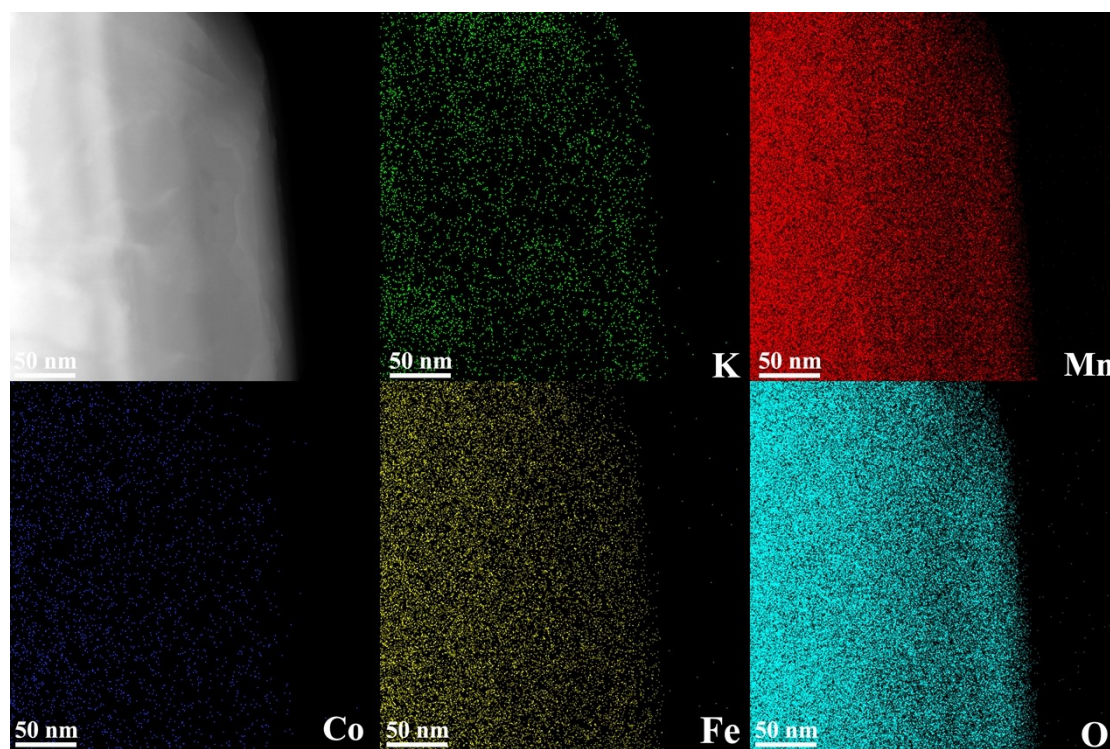


Figure S4. TEM image and the corresponding EDS mapping of the KMCFO.

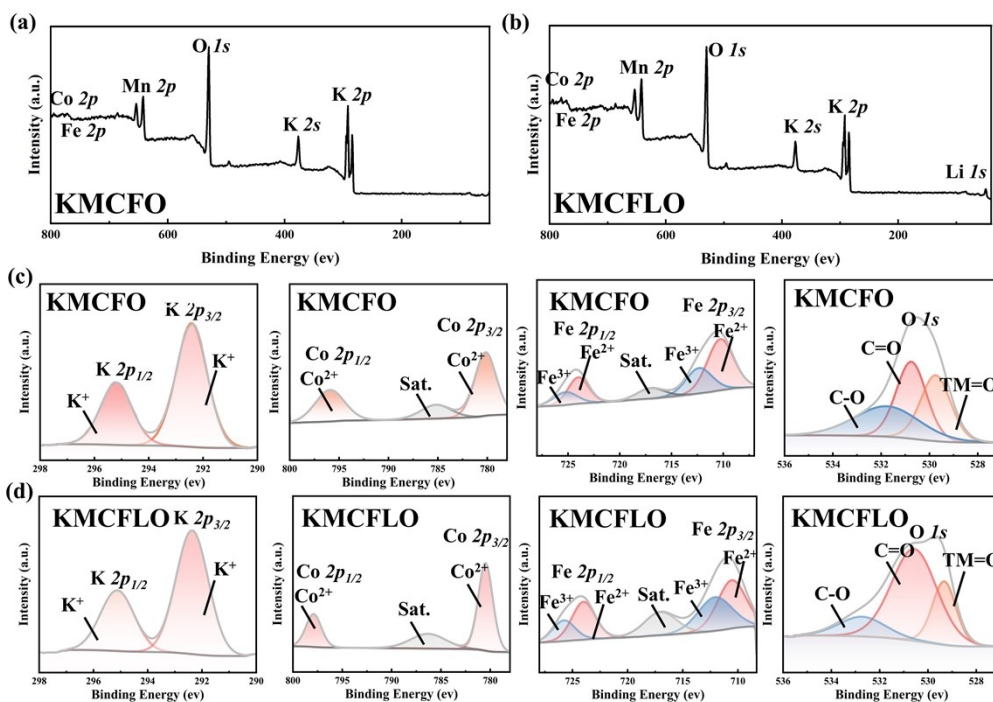


Figure S5. XPS spectra and fitting results: survey spectra of a) KMCFO and b) KMCFLO, c) K 2p, Co 2p, Fe 2p and O 1s of KMCFO, d) K 2p, Co 2p, Fe 2p and O 1s of KMCFLO.

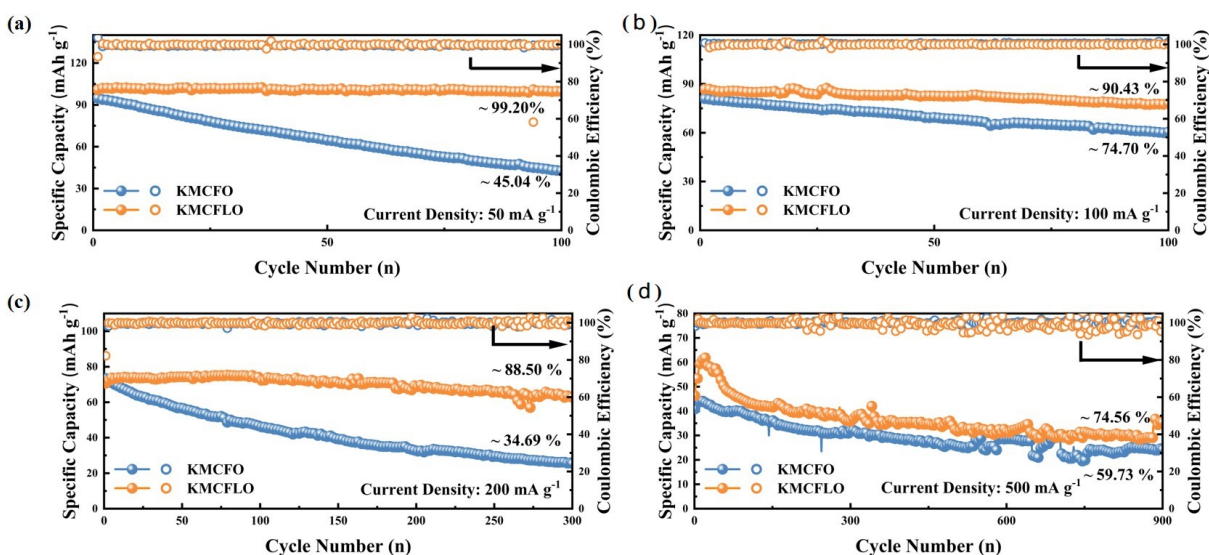


Figure S6. Long-term cycling performance of KMCFO and KMCFLO at a) 50 mA g⁻¹, b) 100 mA g⁻¹, c) 200 mA g⁻¹, d) 500 mA g⁻¹.

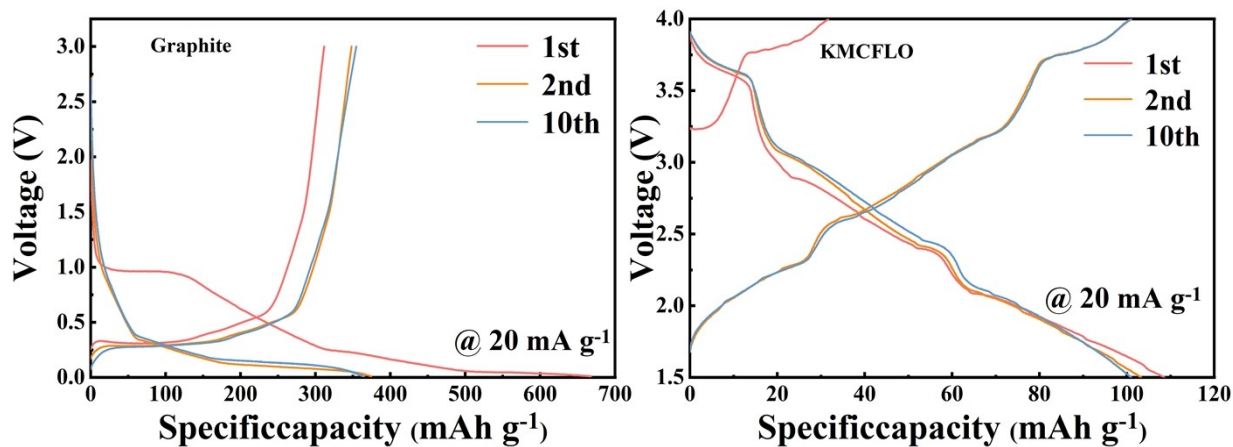


Figure S7. Electrochemical performance of KMCFO and graphite electrodes in half-cells.

Table S1. Structural parameters of KMCFO and KMCFL obtained by Rietveld refinement of Figure 1a.

	a-axis (Å)	c-axis (Å)	R _{wp} (%)	GOF	Space group	ICDD-PDF	Wt%
KMCFO	2.827	20.999	3.85	4.38	R 3 m	16-0205	—
KMCFL	2.886	20.886	7.984	5.78	R 3 m	16-0205	95.1
O	4.929	8.5305					C 2/c

Table S2. Information of the fitting procedure for XPS test results of powder samples.

Samples and Current	Initial Specific Discharge	Number of Cycles	Capacity Retention
Density (mA g ⁻¹)	Capacity (mAh g ⁻¹)	(n)	(%)
KMCFO	20	103.8	68.04
	50	94.7	45.04
	100	80.8	74.70
	200	73.3	34.69
	500	40.8	59.73
KMCFLO	20	107.1	82.36
	50	100.8	99.20
	100	86.8	90.43
	200	70.6	88.50
	500	46.3	74.56

Table S3. Information of the fitting procedure for XPS test results of powder samples.

Samples and Elemental	Position	FWHM Constraint (eV)	Residual Standard
Orbits	Constraint (eV)		Deviation
KMCFLO	K <i>2p</i>	$\Delta_K=2.8$	3.01
	Mn <i>2p</i>	$\Delta_{Mn}=11.2$	1.753
	Co <i>2p</i>	$\Delta_{Co}=14.99$	1.21
	Fe <i>2p</i>	$\Delta_{Fe}=13.1$	1.19
	Li <i>1s</i>	/	1.283
	O <i>1s</i>	/	1.348
KMCFO	K <i>2p</i>	$\Delta_K=2.8$	2.147
	Mn <i>2p</i>	$\Delta_{Mn}=11.2$	1.302
	Co <i>2p</i>	$\Delta_{Co}=14.99$	1.005

Fe $2p$	$\Delta_{\text{Fe}}=13.1$	0.5-3.0	1.136
O $1s$	/	0.5-2.5	0.8965

Table S4. The information on the split fitting peak of XPS tests for Fe $2p$, Co $2p$, K $2p$ and O $1s$ in KMCFO and KMCFLO materials.

Samples and Elemental Orbits	Peak Position of the Fitting Peak (eV)	FWHM Constraint (eV)	
KMCFO	K $2p_{1/2}$	295.19	0.5-2.0
	K $2p_{3/2}$	294.42	0.5-2.0
	Co $2p_{1/2}$	795.93	0.5-2.0
	Co $2p_{3/2}$	780.18	0.5-2.0
	Fe $2p_{1/2}$	724.00, 725.26	0.5-3.0
	Fe $2p_{3/2}$	710.28, 712.33	0.5-3.0
	O $1s$	529.70, 530.75, 531.75	0.5-2.5
	KMCFLO	K $2p_{1/2}$	295.12
K $2p_{3/2}$		292.36	0.5-2.0
Co $2p_{1/2}$		795.17	0.5-2.0
Co $2p_{3/2}$		780.14	0.5-2.0
Fe $2p_{1/2}$		723.99, 725.78	0.5-3.0
Fe $2p_{3/2}$		710.55, 712.07	0.5-3.0
O $1s$		529.3, 530.57, 532.72	0.5-2.5

Table S5. The comparison of electrochemical performances between some reported cathode materials and KMCFL0 in this work.

Cathode	Method	Voltage range	Capacity	Capacity retention
$K_{0.32}MnO_2$	hydrothermal	2.0-4.5V	28.8 mA h g ⁻¹ at 500 mA g ⁻¹	73.37% at 100 mA g ⁻¹ (100 cycles)
$K_{0.44}Ni_{0.22}Mn_{0.78}O_2$	solid-state	1.5-4.0V	58 mA h g ⁻¹ at 500 mA g ⁻¹	67% at 200 mA g ⁻¹ (500 cycles)
$K_{0.3}Mn_{0.95}Co_{0.05}O_2$	sol-gel	2.0-3.6V	99 mA h g ⁻¹ at 22 mA g ⁻¹	75% at 173 mA g ⁻¹ (500 cycles)
$K_{0.6}CoO_2$	solvent-thermal	1.7-4.0 V	40 mA h g ⁻¹ at 200 mA g ⁻¹	87% at 40 mA g ⁻¹ (300 cycles)
$KCrO_2$	solid-state	1.5-4.0 V	31 mA h g ⁻¹ at 500 mA g ⁻¹	67% at 10 mA g ⁻¹ (100 cycles)
$K_{0.5}MnO_2@Al_2O_3$	solvothermal	1.5-4.0 V	95.3 mA h g ⁻¹ at 50 mA g ⁻¹	53% at 50 mA g ⁻¹ (300 cycles)
$K_{0.54}Mn_{0.78}Mg_{0.22}O_2$	solid-state	1.5-4.0 V	96.8 mA h g ⁻¹ at 100 mA g ⁻¹	84% at 100 mA g ⁻¹ (100 cycles)
$K_{0.5}Mn_{0.9}Mg_{0.1}O_2$	solid-state	1.5-4.0 V	102 mA h g ⁻¹ at 10 mA g ⁻¹	21.5% at 100 mA g ⁻¹ (400 cycles)

Table S6. Fitting results of variable temperature electrochemical impedance spectroscopy and apparent activation energy magnitude.

Sample	Temperature (°C)	R_{ct} (Ω)	E_a (KJ mol ⁻¹)
KMCFO	10	37930	84.04
	15	21786	
	20	12844	
	25	7540	
	30	4506	
KMCFO	10	26746	81.55
	15	15734	
	20	8940	
	25	5614	
	30	3207	

Table S7. The peak current at different scan rates and calculation results of D_k .

Sample	Position	Peak current (mA, follow the scan rates of 0.2, 0.5, 1, 2, 5 mV s ⁻¹ , the '-' for discharge)	Slope of the fitting curve	D_k (cm ² s ⁻¹ , '-' for discharge)
KMCFO	Peak 1	0.024, 0.057, 0.133, 0.206, 0.449	0.246	4.49×10^{-10}
	Peak 2	-0.027, -0.058, -0.090, -0.143, -0.254	-0.127	-2.32×10^{-10}
	Peak 3	-0.024, -0.062, -0.098, -0.181, -0.379	-0.126	-2.30×10^{-10}
KMCFO	Peak 1	0.028, 0.071, 0.147, 0.265, 0.581	0.312	5.70×10^{-10}
	Peak 2	-0.036, -0.071, -0.118, -0.219, -0.424	-0.220	-4.02×10^{-10}
	Peak 3	-0.043, -0.100, -0.172, -0.301, -0.621	-0.300	-5.48×10^{-10}